Monthly Notices of the ROYAL ASTRONOMICAL SOCIETY

MNRAS **501,** 1215–1227 (2021) doi:10.1093/mnras/staa3646
Advance Access publication 2020 November 21

Cavezzo, the first Italian meteorite recovered by the PRISMA fireball network. Orbit, trajectory, and strewn-field

D. Gardiol [1]★ D. Barghini [1,2]★ A. Buzzoni,[3] A. Carbognani [3] M. Di Carlo,[4] M. Di Martino,[1] C. Knapic,[5] E. Londero,[5] G. Pratesi,[6,7] S. Rasetti,[1] W. Riva,[8] R. Salerno,[9] G. M. Stirpe,[3] G. B. Valsecchi,[7,10] C. A. Volpicelli,[1] S. Zorba,[5] F. Colas,[11] B. Zanda,[11,12] S. Bouley,[11,13] S. Jeanne,[11] A. Malgoyre,[14] M. Birlan,[11] C. Blanpain,[14] J. Gattacceca,[15] J. Lecubin,[14] C. Marmo,[13] J. L. Rault,[11,16] J. Vaubaillon [11] P. Vernazza,[17] F. Affaticati,[18] M. Albani,[18] A. Andreis,[19] G. Ascione,[20] T. Avoscan,[21] P. Bacci,[22] R. Baldini,[23] A. Balestrero,[8] S. Basso,[24] R. Bellitto,[25] M. Belluso,[26] C. Benna,[1] F. Bernardi,[27] M. E. Bertaina,[2] L. Betti,[28] R. Bonino,[2] K. Boros,[29] A. Bussi,[21] C. Carli,[7] T. Carriero,[1] E. Cascone,[30] C. Cattaneo,[31] A. Cellino [1] P. Colombetti,[2,32] E. Colombi,[33] M. Costa,[8] G. Cremonese,[34] D. Cricchio,[35] G. D'Agostino,[36] M. D'Elia,[37] M. De Maio,[38] P. Demaria,[19] A. Di Dato,[30] R. Di Luca,[3] F. Federici,[39] V. Gagliarducci,[40] A. Gerardi,[40] G. Giuli,[41] D. Guidetti,[42] G. Interrante,[43] M. Lazzarin,[44] S. Lera,[29] G. Leto [26] D. Licchelli,[45] F. Lippolis,[46] F. Manca,[47] S. Mancuso,[1] F. Mannucci,[48] R. Masi,[49] S. Masiero,[35] S. Meucci,[49] A. Misiano,[36] V. Moggi Cecchi [50] E. Molinari,[51] J. Monari,[42] M. Montemaggi,[25] M. Montesarchio,[52] G. Monti,[53] P. Morini,[54] A. Nastasi,[35] E. Pace,[55] R. Pardini,[33] M. Pavone,[56] A. Pegoraro,[57] S. Pietronave,[53] T. Pisanu,[51] N. Pugno,[58] U. Repetti,[21] M. Rigoni,[31] N. Rizzi,[46] C. Romeni,[59] M. Romeo,[36] S. Rubinetti,[60] P. Russo,[20] F. Salvati,[1] D. Selvestrel,[34] R. Serra,[61] C. Simoncelli,[38] R. Smareglia,[5] M. Soldi,[31] R. Stanga,[28] F. Strafella,[37] M. Suvieri,[62] C. Taricco,[2] G. Tigani Sava,[54] M. Tombelli,[43] P. Trivero,[63] G. Umbriaco,[44] R. Vairetti,[64] G. Valente,[65] P. Volpini,[49] R. Zagarella[66] and A. Zollo[52]

Affiliations are listed at the end of the paper

Accepted 2020 November 16. Received 2020 November 9; in original form 2020 September 18

ABSTRACT

Two meteorite pieces have been recovered in Italy, near the town of Cavezzo (Modena), on 2020 January 4th. The associated fireball was observed on the evening of New Year's Day 2020 by eight all-sky cameras of the PRISMA fireball network, a partner of FRIPON. The computed trajectory had an inclination angle of approximately 68° and a velocity at infinity of 12.8 km s^{-1}. Together with the relatively low terminal height, estimated as 21.5 km, those values were indicating the significant possibility of a meteorite dropping event, as additionally confirmed by the non-zero residual total mass. The strewn-field was computed taking into account the presence of two bright light flashes, revealing that the meteoroid had been very likely subject to fragmentation. Three days after the event, two samples, weighing 3.1 and 52.2 g, were collected as a result of a dedicated field search and thanks to the involvement of the local people. The two pieces were immediately recognized as freshly fallen fragments of meteorite. The computed orbital elements, compared with the ones of known Near-Earth Asteroids from the NEODyS database, are compatible with one asteroid only; 2013 VC_{10}. The estimated original mass of the meteoroid, 3.5 kg, and size, approximately 13 cm, is so far the smallest among the current 35 cases in which meteorites were recovered from precise strewn-field computation thanks to observational data. This result demonstrates the effectiveness of accurate processing of fireball network data even on challenging events generated by small size meteoroids.

Key words: methods: data analysis – techniques: image processing – meteorites, meteors, meteoroids.

1 INTRODUCTION

The analysis of meteoritic material plays a relevant role in modern planetary sciences, since the fall of meteorites provides the easiest and cheapest way to gather extra-terrestrial samples. The mineralogy

★ E-mail: daniele.gardiol@inaf.it (DG); dario.barghini@inaf.it (DB)

© 2020 The Author(s)
Published by Oxford University Press on behalf of Royal Astronomical Society

Downloaded from https://academic.oup.com/mnras/article/501/1/1215/5998250 by Biblioteca Scienze Tecnologiche user on 21 March 2022

and petrology of these samples are the major sources of information about the geology, formation, and evolution of minor and major bodies in the Solar system and beyond (e.g. Kruijer, Kleine & Borg 2020 and references therein). The scientific importance of such material is even higher if the interaction of the body with the Earth's atmosphere, generating the meteorite falls, is observed. Firstly, the observation of the meteor can provide crucial information about the physical properties of the body entering the atmosphere, which usually ablates for the most part before reaching the ground, if anything survives. In this case, the knowledge of the orbit of the meteoroid unveils its origin in the Solar system which can be linked with the physical and chemical characterization of the meteorite itself. At this time of writing, the Meteoritical Database[1] lists almost 64 000 officially classified meteorites. Among them, to the authors' knowledge, only 35 (plus at least 2 not yet published) were collected together with a sufficient set of observations of their atmospheric path, allowing a reliable reconstruction of their heliocentric orbit before the interaction with the Earth's atmosphere. Gathering sufficient statistics for meteoroid orbits would enable investigations into the possible link between different meteorite classes and their origin in the Solar system. Ultimately, the knowledge of the source regions of particular meteorite groups can provide constraints for the identification of a common parent body. As an example of recent relevant results on this topic, the reader can refer to Granvik & Brown (2018), Jenniskens et al. (2019), and Unsalan et al. (2019). The importance of such results for planetary science is so pronounced that efforts even have been made to reconstruct meteorite pre-impact orbits from historical records (Gounelle, Spurný & Bland 2006).

The case of the Pribram meteorite in 1959 (Ceplecha 1961) represents the first successful meteorite recovery resulting from the observation of a bright meteor, which allowed for precise computation of its atmospheric trajectory, dynamics, and dark flight. At the same time, this was the first meteorite recovery carried out thanks to a systematic meteors observation survey. Following the example of the Czechoslovakian Fireball Network, now European Fireball Network (Spurný et al. 2017b), many dedicated projects started to realize observational networks. Run by both amateur and professional astronomers, these networks have a shared goal of continuously monitoring the night-sky and detecting meteor and fireball events. The scientific outcome for this kind of survey is twofold; providing a unique tool to discover new meteor showers by focusing on the faint but predominant component of the detected events, and capturing the very rare occurrence of meteorite-dropping fireballs. In this context, one should highlight that only 20 among the 35 'pedigree' meteorites were collected as a result of dedicated observational surveys (see Table 1). Excluding the well-known but out-of-range events of Almahata Sitta and Chelyabinsk, the remaining 13 falls were documented through sporadic observations only, such as security cameras, dash cams, and visual reports. For this reason, the past few years have witnessed a remarkable and ever increasing effort to extend the coverage of meteor networks worldwide and maximize the efficiency in the recovery of meteorites. As a result, 9 among the 20 meteorites collected, thanks to meteor surveillance networks, were recovered most recently between 2014–2020.

In this international scenario, the PRISMA all-sky camera network (Gardiol, Cellino & Di Martino 2016; Gardiol et al. 2019) was born in 2016 to achieve a systematic surveillance of meteors and fireballs in the skies over the Italian territory. In fact, PRISMA stands for 'Prima Rete Italiana per la Sorveglianza sistematica di Meteore e Atmosfera' (First Italian Network for Meteors and Atmosphere systematic Surveillance). At this time of writing, PRISMA has deployed 52 stations, among which 37 are fully operating and 15 are in installation phase. The PRISMA project is part of the international collaboration initiated by the FRIPON project (Fireball Recovery and InterPlanetary Observation Network, Colas et al. 2014; Jeanne et al. 2019; Colas et al. 2020).

In this paper, we report on the finding of two meteorite pieces in Italy, near the Cavezzo village (Modena, Emilia-Romagna). The meteorite-dropping fireball, which reached a brightest absolute magnitude of −9.5, was observed on the evening of New Year's Day 2020 by eight all-sky cameras of the PRISMA network. The two fragments, weighing 3.1 and 52.2 g, respectively, were collected as a result of a dedicated field search and thanks to the involvement of the local people. In Section 2, we illustrate the preliminary strewn-field computation and the meteorite search activity, and give a short description of the two recovered fragments. Section 3 gives a complete review of the fireball data analysis and its physical characterization. In Section 4, we provide the orbital parameters and discuss a possible progenitor for the observed meteoroid. We draw our conclusions in Section 5.

2 THE FIREBALL EVENT

2.1 Preliminary trajectory and strewn-field

On January 1st at 18:26:53 UT, eight stations of the PRISMA network detected a brilliant fireball, named IT20200101, in the skies of northern Italy (the list is shown in Table 2). The FRIPON automatic alert system performed a preliminary data reduction based on four cameras (ITPI03, ITTO02, ITER04, ITVE02). The remaining cameras were not configured to work as part of the automatic data reduction pipeline, having being installed just prior to the detection. These preliminary results indicated a high probability of a meteorite-dropping fireball, as the computed pre-atmospheric velocity was found to be about 12 km s^{-1} and the inclination of the trajectory was high (68°). The meteor was tracked down to a height of about 22 km, and the light curve showed two sudden brightenings at altitude of about 32 and 30 km. In order to get a preliminary estimate of the strewn-field, we reprocessed the data manually, adding two of the missing cameras (ITLO03 and ITER01). In the meantime, we also started to receive many reports from visual observers (52 observations reported through the PRISMA website on the International Meteor Organization online form[2]).

The high angle of fall resulted in an intense ablation process that led the fireball to shine with a mean absolute visual magnitude of about −7.5. The fireball disappeared from the camera images at an altitude of about 21.5 km. According to the first computation of the strewn-field, made using a purely ablative model, we estimated a nominal impact point close to the village of Disvetro in the municipality of Cavezzo (province of Modena), near the local astronomical observatory, in the middle of the Po Valley. However, the light-curve profile suggested that the object underwent a fragmentation process during the atmospheric flight, as also supported by eyewitnesses. Therefore, we expected meteorite pieces to be spread around the line joining Disvetro with the on-ground projection of the final part of the visible trajectory, near the village of Rovereto sulla Secchia.

[1]The Meteoritical Society, https://www.lpi.usra.edu/meteor/

[2]https://prisma.imo.net/members/imo_view/event/2020/18

Downloaded from https://academic.oup.com/mnras/article/501/1/1215/5998250 by Biblioteca Scienze Tecnologiche user on 21 March 2022

Table 1. List and relevant data of 'pedigree' meteorites, i.e. for which recovery was accompanied by a sufficient set of sporadic or systematic observations (optical, radio, infrasound, seismic, satellite), allowing for pre-impact orbit reconstruction. From left- to right-hand side: name of the meteorite (approved by The Meteoritical Society), date of fall, preatmospheric velocity and mass, estimated terminal mass, meteorite total known weight (TKW) recovered on the ground, minimum absolute magnitude recorded, impact energy (equivalent tons of TNT, 1 T = 4.187×10^9 J), fireball network which provided the observations (if any) and references for table data. The uncertainties associated to the values of the table are not given here for simplicity, but can be found in the respective references.

Name	Date UT	v_∞ (km s^{-1})	m_∞ (kg)	m_{fin} (kg)	TKW (kg)	M[a]	E (T)[b]	Fireball Network[c]	References
Příbram	07/04/1959	20.9	1300	80	5.6	−19	70	CFN	1, 2
Lost City	04/01/1970	14.1	165	25	17	−12	4	PFN	3, 4, 5
Innisfree	06/02/1977	14.7	42	4.9	4.58	−12.1	1	MORP	5, 6
Benešov	07/05/1991	21.3	4100	300[d]	0.0116	−19.5	200	EFN	5, 7, 8, 9
Peekskill	09/10/1992	14.7	5000	–	12.4	−16	130	–	2, 10
Tagish Lake	18/01/2000	15.8	56000	1300	10	−22	1700	–	11, 12, 13
Morávka	06/05/2000	22.5	1500	100	1.4	−20	90	–	14, 15, 2
Neuschwanstein	06/04/2002	20.9	300	20	6.22	−17.2	16	EFN	16, 17, 18
Park Forest	27/03/2003	19.5	11000	–	30	−21.7	500	–	19, 20
Villalbeto de la Peña	04/01/2004	16.9	600	13	5.2	−18	20	–	21, 22, 23
Bunburra Rockhole	20/07/2007	13.4	22	1.1	0.339	−9.6	0.5	DFN	24, 25
Almahata Sitta	07/10/2008	12.4	40000	39	10.7	−19.7	730	–	26, 27, 28, 29
Buzzard Coulee	21/11/2008	18.0	10000	–	>200	−20	390	–	30, 31, 32
Maribo	17/01/2009	28.3	2000	<20	0.0258	−20	190	–	33, 34
Jesenice	09/04/2009	13.8	170	20	3.611	−15	4	SFN	35, 36
Grimsby	26/09/2009	20.9	30	5	0.215	−14.8	2	SOMN	37
Košice	28/02/2010	15.0	3500	500	11.3	−18	100	–	38, 39
Mason Gully	13/04/2010	14.5	40	–	0.0245	−9.4	1	DFN	40, 41
Križevci	04/02/2011	18.2	50	<5[e]	0.291	−13.7	2	CMN	42
Sutter's Mill	22/04/2012	28.6	40000	–	0.943	−19	4000	–	43
Novato	18/10/2012	13.7	80	–	0.363	−13.8	3	CAMS	44
Chelyabinsk	15/02/2013	19.0	$1.2 \cdot 10^7$	10000	730	−27.3	$5 \cdot 10^5$	–	45, 46, 47
Annama	18/04/2014	24.2	470	12.5	0.1679	−18.3	30	FFN	48, 49, 50
Žďár nad Sázavou	09/12/2014	21.9	150	>1.3[f]	0.087	−15.3	9	EFN	51
Porangaba	09/01/2015	–	–	–	0.970	–	–	–	52
Sariçiçek	02/09/2015	17.3	1700	–	24.78	−16.8	60	–	53
Creston	23/10/2015	16.0	50	–	0.8523	−12	2	CAMS, SACN	54
Murrili	27/11/2015	13.7	38	2	1.68	–	0.9	DFN	55, 56
Ejby	06/02/2016	14.5	120	–	8.982	−14.0	3	–	57, 58
Stubenberg	06/03/2016	14	600	–	1.473	−15.5	14	EFN	59, 60
Hradec Králové	17/05/2016	–	–	–	0.134	−11.5	–	EFN	61, 62
Dishchii'bikoh	02/06/2016	16.6	1000[g]	–	0.07957	−16	30	CAMS, SACN	63, 64
Dingle Dell	31/10/2016	15.4	40	1.4	1.150	–	1	DFN	65
Hamburg	17/01/2018	15.8	140	>1	∼1	−16.3	5.5	–	66, 67
Renchen	10/07/2018	20	50[h]	–	1.227	−13.4	2	EFN	61, 68
Cavezzo	01/01/2020	12.8	3.5	1.5	0.0553	−9.5	0.07	PRISMA	This work

Notes. [a] Magnitude values are given in different passbands (e.g. visual, panchromatic) and might be not strictly comparable to one another. [b] The impact energy was calculated by the authors, if not provided in the original work, or updated to more precise estimates of preatmospheric mass and/or velocity. [c] CFN = Czechoslovakian Fireball Network (now EFN), PFN = Prairie Fireball Network, MORP = Meteorite Observation and Recovery Project, EFN = European Fireball Network, DFN = Desert Fireball Network, SFN = Slovakian Fireball Network (part of EFN), SOMN = Southern Ontario Meteor Network, CMN = Croatian Meteor Network (part of EFN), CAMS = Cameras for All-sky Meteor Surveillance, FFN = Finnish Fireball Network, SACN = Spalding Allsky Camera Network, SkySentinel. [d] Most of the terminal mass in gram-sized meteorites. [e] Apart from the main mass, just a few 10–100 g meteorites are expected and ∼2000 meteorites with mass > 1 g. [f] Main mass of 1.3 kg plus a second largest meteorite in the range 100–200 g (∼250 meteorites in the range 10–200 g, 6 kg total, and ∼3000 meteorites of 0–1 g, 7 kg total). [g]There is a disagreement between meteoroid size deduced from radiated energy from satellite observations (∼15 000 kg) and cosmogenic radionuclide data (400–1800 kg). [h] Computed by the authors considering a preatmospheric radius of 10–20 cm deduced from cosmogenic ^{26}Al data and a bulk density of 3.4 g cm^{-3} (reference 68), assuming a spherical shape.

References: [1] Ceplecha (1961) [2] Borovička & Kalenda (2003) [3] McCrosky et al. (1971) [4] Ceplecha (1996) [5] Ceplecha & Revelle (2005) [6] Halliday, Griffin & Blackwell (1981) [7] Spurný (1994) [8] Borovička et al. (1998) [9] Spurný et al. (2014) [10] Brown et al. (1994) [11] Brown et al. (2000) [12] Brown et al. (2002) [13] Hildebrand et al. (2006) [14] Borovička et al. (2003a) [15] Borovička et al. (2003b) [16] Spurný, Heinlein & Oberst (2002) [17] Spurný, Oberst & Heinlein (2003) [18] Revelle, Brown & Spurný (2004) [19] Simon et al. (2004) [20] Brown et al. (2004) [21] Llorca et al. (2005) [22] Trigo-Rodríguez et al. (2006) [23] Bischoff et al. (2013) [24] Bland et al. (2009) [25] Spurný et al. (2012) [26] Jenniskens et al. (2009) [27] Borovička & Charvát (2009) [28] Shaddad et al. (2010) [29] Welten et al. (2010) [30] Hildebrand et al. (2009) [31] Milley et al. (2010) [32] Wilson & McCausland (2012) [33] Haack et al. (2012) [34] Borovička, Popova & Spurný (2019) [35] Spurný et al. (2010) [36] Bischoff et al. (2011) [37] Brown et al. (2011) [38] Borovička et al. (2013a) [39] Tóth et al. (2015) [40] Spurný et al. (2011) [41] Dyl et al. (2016) [42] Borovička et al. (2015) [43] Jenniskens et al. (2012) [44] Jenniskens et al. (2014) [45] Popova et al. (2013) [46] Borovička et al. (2013b) [47] Brown et al. (2013) [48] Trigo-Rodríguez et al. (2015) [49] Kohout et al. (2017) [50] Bouvier et al. (2017) [51] Spurný, Borovička & Shrbený (2020) [52] Ferus et al. (2020) [53] Unsalan et al. (2019) [54] Jenniskens et al. (2019) [55] Bland et al. (2016) [56] Sansom et al. (2020) [57] Spurný et al. (2017a) [58] Haack et al. (2019) [59] Spurný et al. (2016) [60] Bischoff et al. (2017) [61] Spurný et al. (2019) [62] Gattacceca et al. (2019) [63] Palotai et al. (2019) [64] Jenniskens et al. (2020) [65] Devillepoix et al. (2018) [66] Brown et al. (2019) [67] Gattacceca et al. (2020) [68] Bischoff et al. (2019).

Downloaded from https://academic.oup.com/mnras/article/501/1/1215/5998250 by Biblioteca Scienze Tecnologiche user on 21 March 2022

Table 2. PRISMA stations that observed the IT20200101 fireball. From left to right: station name, latitude, longitude, and elevation above sea level.

Station name	Lat. N [°]	Long. E [°]	El. [m]
Bedonia (ITER04)	44°30′27.″7	09°37′57.″0	550
Rovigo (ITVE02)	45°04′54.″0	11°47′42.″2	15
Felizzano (ITPI03)	44°54′45.″0	08°26′14.″0	114
Loiano (ITER01)	44°15′23.″7	11°19′54.″4	787
Cecima (ITLO03)	44°48′52.″7	09°04′43.″6	670
Navacchio (ITTO02)	43°40′59.″5	10°29′29.″9	15
Padova (ITVE01)	45°24′07.″0	11°52′06.″7	64
Asiago (ITVE03)	45°50′57.″9	11°34′06.″0	1370

2.2 Meteorite search and recovery

As soon as the preliminary strewn-field was identified (the day following the fall, i.e. January 2nd in the early afternoon), we had to decide a strategy for the meteorite search. Within the PRISMA collaboration, a team of volunteers, both professionals and amateurs, is trained for meteorite hunting and dedicated to search activities. The strewn-field, located between the towns of Rovereto sulla Secchia and Disvetro, lies in a rural territory with many cultivated fields, groves and houses spread over the area. Since the vast majority of the terrain is private property, we notified the local authorities that teams of hunters would be there to search for meteorites on behalf of the PRISMA collaboration. To help searchers enter private terrains and areas, we also involved the Civil Protection of Cavezzo, as they are usually employed during public events, and their members are well known among the community. At the same time, we prepared a press release to be published on the PRISMA website[3] and on the outreach platform of INAF (MediaINAF[4]). In the press release, we provided all the necessary information about the most probable area where fragments could be found and also a brief tutorial on how to recognize a freshly fallen meteorite. The goal of this strategy was to maximize the probability of a successful recovery by involving a larger number of people, even if not specially trained. The press release was also sent to local media in the Modena area, encouraging local inhabitants to start their own search or at least to be aware that they might chance upon meteorite fragments, and in this case to contact us by email. The news was made public on the late afternoon of January 2nd, and already on January 3rd, we started receiving reports from people in the local area and giving interviews to local and national newspapers and televisions. By the morning of January 4th, a team of about twenty hunters was ready to start searches on Sunday 5th, while a small scouting group from Bologna University led by Romano Serra was already on-site. On January 4th at 3 PM local time, we received an email with the first reliable meteorite candidate from Mr. Davide Gaddi, reporting the recovery of a small fragment (the size of a fingernail) on an embankment along the Secchia river. We immediately arranged a meeting with Romano Serra, where Mr. Gaddi showed also a second larger fragment, found in the meantime in the same place, the size of a walnut. Both fragments were recognized to be freshly fallen meteorites. It was less than three days since the fireball event.

[3]http://www.prisma.inaf.it/index.php/2020/01/02/una-meteorite-in-emilia-romagna

[4]https://www.media.inaf.it/2020/01/02/forse-e-caduta-una-meteorite-in-emilia-romagna

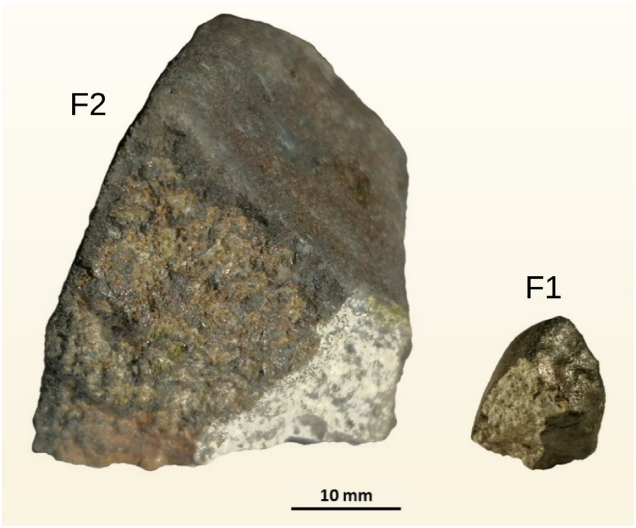


Figure 1. The two recovered samples of the Cavezzo meteorite. On the right-hand side, the first recovered fragment (F1, 3.1 g); on the left-hand side, the second and larger one (F2, 52.2 g).

In the following days, the search for other fragments carried out by teams organized by PRISMA and by other people did not lead to further findings, even though a refined strewn-field was available in the meantime.[5] Bad weather and muddy fields also limited the area accessible for the search. We planned to resume searches in Spring 2020 hoping for better weather and terrain conditions but, up until now, the COVID-19 pandemic outbreak did not allow us to organize further on-field activities.

2.3 Meteorite fragments description

The two fragments were recovered at coordinates 44°49′43.″7 N 10°58′19.″5 E, at the border of a narrow country road that runs parallel to the left main embankment of the Secchia river. This is approximately halfway between Villa Motta and Rovereto sulla Secchia in the territory of the municipality of Cavezzo. Fig. 1 shows the two finds. Fragment n.1 (F1), the first one to be found, has a tetrahedral form and weighs 3.1 g. Fragment n.2 (F2), the largest one, weighs 52.2 g. Both fragments clearly present a recently formed fusion crust on most of their surface. They also show what appears to be a light grey chondritic pattern on one of their sides, which was probably due to fragmentation that most likely occurred when they hit the ground. This interpretation is corroborated by the presence of an impact feature that is visible on one of the edges separating two of their sides, also accompanied by white streaks (Fig. 2a). In addition, F2 presents a darker grey colouration on one side, apparently a less pronounced secondary fusion crust, which is compatible with exposure due to a fragmentation event most probably associated to the brightening which occurred at a height of around 30 km.

The meteorite fragments are currently being analysed at the Department for Earth Science of the Firenze University for classification and study of the mineralogical, petrographic, and geochemical characteristics. The result of this extensive analysis will be the subject of a dedicated article. However, as for fragment F2, it is worth

[5]PRISMA and FRIPON teams independently computed two strewn-fields that are in close agreement with each other.

Downloaded from https://academic.oup.com/mnras/article/501/1/1215/5998250 by Biblioteca Scienze Tecnologiche user on 21 March 2022

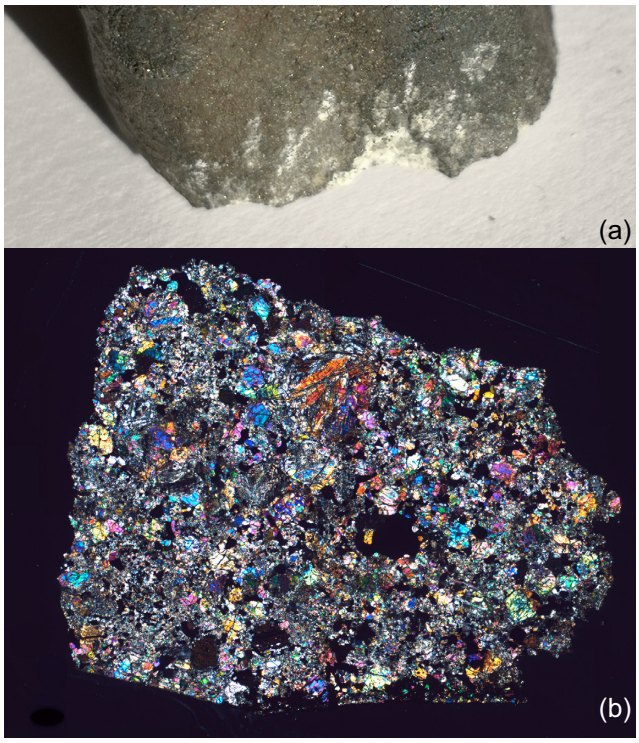


Figure 2. Details of the larger fragment F2 of the Cavezzo meteorite. (a) White streaks occur on one edge of F2, suggesting on-ground breakup of the original body; (b) photomosaic of polarizing optical microscope images (transmitted light, crossed polars) of a thin sections obtained from F2 (field width 12 mm) showing chondrules and chondrule fragments distributed in the matrix.

mentioning that the composition of olivine and low-Ca pyroxene, the abundances of the mineral phases and the texture (Fig. 2b) are fully compatible with the L chondritic group. On the other hand, the modal mineralogy of fragment F1 (namely, the extremely low content of iron and troilite and the very high abundance of high-Ca pyroxene) is clearly different from the one typically found in L chondrites. On 2020 September 5th, the Nomenclature Committee of the Meteoritical Society has approved the classification proposal of 'L5 anomalous' chondrite. Cavezzo is the only approved meteorite belonging to this class.[6] Fig. 2b shows a photomosaic of polarizing optical microscope images of a thin section obtained from F2, where, distributed in the matrix, chondrules and chondrule fragments can be observed.

The γ-ray activity measurement performed on the F2 sample at the INAF Monte dei Cappuccini Laboratory in Torino (Taricco et al. 2006, Colombetti et al. 2013) has shown the presence of many cosmogenic radioisotopes. Despite the small mass of F2 with respect to the samples that are commonly measured at this facility, the two characteristic lines of ^{48}V at 983.53 and 1312.11 keV[7] are clearly visible, confirming beyond any doubt the presence of this radioisotope. Since ^{48}V has a half-life of 15.97 d, this is an indisputable proof of the very recent fall of the recovered meteorite, thus linking it again to the New Year's fireball. The results of the radiometric measures of F2 will be the subject of a forthcoming publication.

[6]https://www.lpi.usra.edu/meteor/metbull.php?code=72534
[7]NUDAT database – https://www.nndc.bnl.gov/nudat2/

3 FIREBALL DATA ANALYSIS

PRISMA, as a partner of the FRIPON collaboration, currently shares the same technology of the network. Each station is equipped with a CCD camera (6 mm diagonal, 1296 x 966 pixel), coupled with a short focal lens objective (1.25 mm), to obtain an all-sky field of view (FOV). The camera is connected to a Linux operating mini-PC via LAN and controlled by the open-source FREETURE software (Audureau et al. 2014). The camera is operated at 30 fps (1/30 s exposure time) in order to sample the meteor trail with a suitable rate. The meteor detection is triggered locally in each node by a frame difference method, and cross-correlated with respect to data of other nodes to check for multiple detections of the same event. The 30 fps video stream of the detected meteor is saved locally as FITS files and, in the case of a multiple detection, it is collected by the FRIPON central server, located at the Laboratoire d'Astrophysique de Marseille (LAM). Station monitoring, network security, software maintenance, real-time data processing, and sharing tasks are in charge of FRIPON and LAM teams. PRISMA data are synchronized and stored at the IA2 (Italian Center for Astronomical Archives) INAF archiving facilities in Trieste (Knapic et al. 2014). The PRISMA reduction pipeline is developed at the INAF – Osservatorio Astrofisico di Torino and INAF – Osservatorio di Astrofisica e Scienze dello Spazio in Bologna. It is implemented in IDL[8] v8.7 and MATLAB[9] Release 2015b.

The first step in the analysis of meteor detections is the astrometric and photometric reduction. Since almost no stars arise from the background noise in the 30 fps video stream, the control software acquires a 5 s exposure image, named *capture*, every 10 min. With a limiting V magnitude of about +4.5 on this set of images, available for each operational night, hundreds of stars per frame are automatically identified and correlated with catalogue positions. They are then used as a reference for both astrometric and photometric calibration. Concerning astrometry, we implemented the approach introduced by Ceplecha (1987), Borovička (1990), and Borovička, Spurný & Keclikova (1995), in which the absolute astrometric solution of the camera is derived, in the alt/az system, as a function of eight parameters. This analytical description accounts for the major distortion factors that are, in the case of PRISMA all-sky cameras, the pronounced radial distortion of the fish-eye lens and the possible mismatch of the optical centre with respect to the local zenith direction. Two additional parameters are introduced if the optical plate is found to be misaligned with respect to the local horizon plane. With respect to Borovička et al. (1995), we provided a new explicit parametrization of the astrometric model, which reduces the parameters' correlation degree and improves overall convergence properties for the determination of the astrometric solution (Barghini et al. 2019b). At the same time, the photometric calibration is determined on the same set of images as well. Since no filter is applied over the lens, a wide passband magnitude is considered, roughly between 400 and 800 nm, on the basis of the quantum efficiency of the camera and the transmission of the glass dome. This panchromatic magnitude is numerically computed from the catalogue *UBVRI* Johnson-Cousins system and therefore used to derive the zero-point and atmospheric extinction coefficient for each capture. For PRISMA cameras, we also determined and accounted for the efficiency loss along the radial direction that turns out to be

[8]IDL – Interactive Data Language – Harris Geospatial Solutions, Inc. – https://www.harrisgeospatial.com/
[9]MATLAB – Matrix Laboratory – MathWorks, Inc., – http://www.mathworks.com

Downloaded from https://academic.oup.com/mnras/article/501/1/1215/5998250 by Biblioteca Scienze Tecnologiche user on 21 March 2022

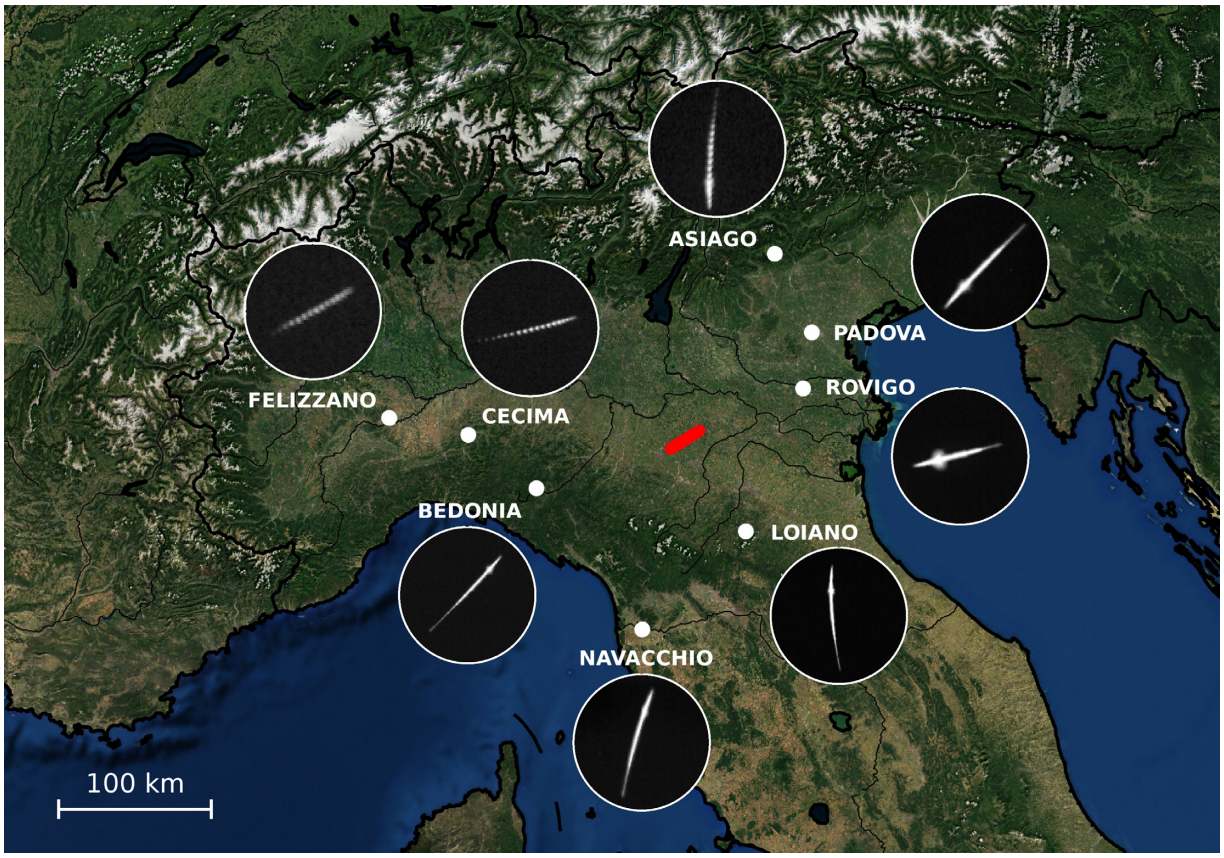


Figure 3. Map of the PRISMA stations (white dots) involved in the detection of the IT20200101 fireball. The red line plots the fireball bright trajectory projected on the ground, and white circles enclose the fireball trail seen by each camera (reconstructed from video records). Please notice that fireball trails are oriented accordingly to the specific in-situ hardware installation, and may be not strictly consistent with one another (all-sky images, from which meteor trails are cropped, were approximately oriented with N direction upward and E direction rightward). Background map was generated using the Matplotlib Basemap Toolkit (Hunter 2007, https://matplotlib.org/basemap/users/index.html).

of about 40 per cent from the centre to the very edge of the camera (Barghini, Gardiol & Carbognani 2019a).

We used the method outlined in Carbognani et al. (2020) to estimate the fireball atmospheric trajectory, its main physical parameters, and the best kinematic parameters in the terminal point of the luminous path. The atmospheric trajectory computation is performed according to the classical formulation reported in Ceplecha (1987) and Borovička (1990). The parameters of the dynamical model are derived based on the description given by Kalenichenko (2006) and references therein. In our case, however, the meteoroid has been most probably subject to fragmentation phenomena, so that the physical quantities are to be taken with caution. For the dark flight and strewn-field determination, Ceplecha (1987) formulation is again used, by computing the expected impact points in a range of mass-section ratios. The orbital parameters are derived both in an analytical way and by numerical integration, as the two methods have proven to provide consistent results (Clark & Wiegert 2011).

3.1 Astrometry and photometry

Fig. 3 shows the map of PRISMA stations that detected the IT20200101 fireball (white dots) together with the on-ground projection of the reconstructed trajectory (red line) and the images of the meteor trail seen by each camera (enclosed in white circles) obtained through the analysis of video records. The distance between the eight stations and the fireball atmospheric trajectory spans between 75 and 200 km. While some cameras captured the bright flight in the central area of the FOV, other cameras recorded the fireball at a quite low elevation above the horizon. In particular, the astrometric reduction for data of two cameras (Felizzano and Cecima) results in elevations lower than 10° for the final 5–10 points of the trajectory. Unfortunately, sky quality condition is not optimal in many PRISMA observational sites, due to light pollution which is especially severe in the Po valley. These experimental constraints prevent us from detecting stars, below 10° of elevation for most PRISMA cameras, even in long-exposure calibration images. While residual systematic effects are numerically addressed (Barghini et al. 2019b), this correction can be only tentative below 10° of elevation and the positional accuracy for these last points is questionable. To assess the potential effect of this bias over the final result, we first excluded these points and verified that the overall results (i.e. the trajectory computation) were unchanged within the measurement errors. In fact, their total weights are not predominant over other reference points, at the same timing, from the remaining six cameras. We finally included them since they provide important photometric data for the trailing edge of the fireball light curve.

The photometric analysis highlights that the fireball point spread function (PSF) saturated, in almost all cameras, between 2 and 4.7 s from the beginning of the bright flight. Barghini et al. (2019b) give a comprehensive analysis of the effects of PSF saturation for PRISMA cameras concluding that the astrometric precision is not significantly degraded at least below $h \leq 4$, where h is the relative ratio of the PSF

Downloaded from https://academic.oup.com/mnras/article/501/1/1215/5998250 by Biblioteca Scienze Tecnologiche user on 21 March 2022

Table 3. IT20200101 fireball parameters obtained from triangulation and dynamical model. The two columns refer to values at the beginning and end of the bright flight, respectively (when applicable). Values of mass and diameter are computed from the mass-section ratio D (in the hypothesis of pure ablation) by assuming a spherical shape of the meteoroid and for the measured meteorite bulk density of 3.322 g cm^{-3}.

		Beginning	Terminal
Time (UT)	t	18:26:52.9	18:26:58.5
Height (km)	h	75.9 ± 0.2	21.5 ± 0.1
Latitude (N)	ϕ	$44^\circ44'03'' \pm 7''$	$44^\circ50'24'' \pm 7''$
Longitude (E)	λ	$10^\circ43'09'' \pm 7''$	$10^\circ57'25'' \pm 7''$
Velocity (km s^{-1})	v	12.2 ± 0.2	4.0 ± 0.2
Mass–section ratio (kg m^{-2})	D	280 ± 20	210 ± 20
Mass (kg)	m	3.5 ± 0.8	1.5 ± 0.4
Diameter (m)	d	0.13 ± 0.01	0.09 ± 0.01
Luminous path-length (km)	L	59	
Duration (s)	T	5.6	
Trajectory inclination (°)	T_i	68.4 ± 0.3	
Trajectory azimuth (°)	az	238.1 ± 0.2	
Min. absolute magnitude	M	-9.5 ± 0.5 @ 32.6 km	
Pre-atmospheric velocity (km s^{-1})	v_∞	12.8 ± 0.2	
Ablation coefficient (s^2 km^{-2})	σ	0.012 ± 0.003	
Max. dynamic pressure (MPa)	P_{max}	1.0 ± 0.3 @ 28.2 km	
Impact Energy (T TNT)	E	0.07 ± 0.02	

height to the saturation value, namely 4095 ADU (analogue-to-digital units) for PRISMA 12-bit video records. To account for count loss on the saturated portion of the PSF, a tentative correction is applied by fitting a bi-dimensional Gaussian model to non-saturated pixels of the PSF. This analysis therefore aims to estimate the original PSF shape and unveils h values that are mostly below 2 (and always below 4), also for the two bright flares (Section 3.2). These conclusions are confirmed by a visual inspection of the saturated portion of the PSF, which is confined to few pixels in its very centre for most part of the trajectory. From this approach, a saturation correction factor is therefore estimated and applied to results obtained through aperture photometry. The computed count loss fraction for the saturated portion of the bright flight is mostly confined under 30 per cent and raises up to about 50 per cent in correspondence of the brightest flare.

3.2 Atmospheric trajectory and dynamical model

The results of the atmospheric trajectory and dynamical model computation are summarized in Table 3 and Fig. 4. In particular, Fig. 4a shows the height of the fireball above the ground as a function of time since the beginning of the luminous path. The observed fireball trajectory begins at a starting height $h_b = 75.9 \pm 0.2$ km and ends up at a terminal height $h_t = 21.5 \pm 0.1$ km. The total length of the luminous atmospheric path is approximately 59 km, which was covered in about 5.6 s. The meteoroid followed an atmospheric trajectory inclined by an angle of $68.^\circ4 \pm 0.^\circ3$ with respect to the horizontal plane, with an azimuth of $238.^\circ1 \pm 0.^\circ2$, travelling from WSW to ENE, and rapidly entered into the denser layers of the atmosphere. The height residuals of observed points with respect to the computed trajectory are plotted in Fig. 4b. The standard deviation of $\sigma_h = 0.25$ km, considering the distance of the fireball to the observing stations, corresponds to angles less then 10 arcmin and it is therefore always below the pixel resolution of our cameras. Systematic patterns are visible along the trajectory. Above 50 km of altitude, the descent of the body into the atmosphere is slower in comparison to the fitted trajectory. Furthermore, after the two flare events, an increased spreading of the height residuals is evident.

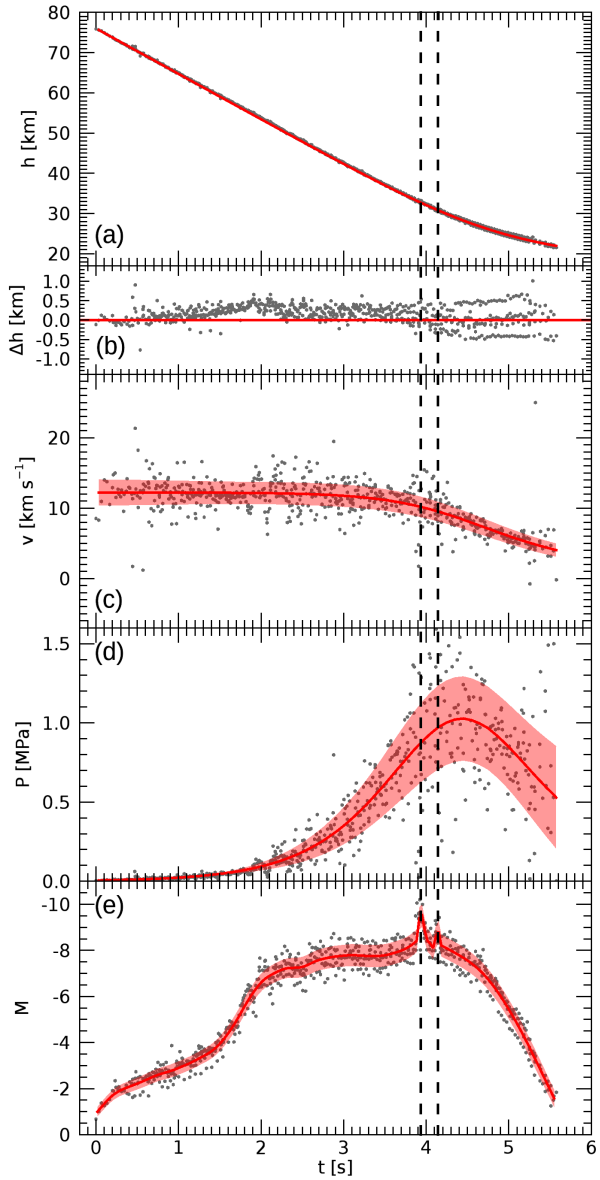


Figure 4. Results of trajectory computation and dynamical model for the IT20200101 fireball. (a) Vertical projection of the atmospheric trajectory; (b) vertical residuals of the atmospheric trajectory; (c) fireball velocity with respect to ground; (d) aerodynamic pressure (Equation 1); (e) absolute magnitude (at 100 km, zenith of the observer). The x-axis reports the time elapsed from the beginning of the visible flight captured by the eight cameras. The two vertical dashed lines indicate the times at which the two flares occurred, 3.95 and 4.15 s, respectively. In every panel, grey points plot measured or computed values for the single stations, whereas the red line plots the nominal fit values (a–c) or a smoothed version of grey points (d,e). Red shaded area encloses 1σ uncertainty.

Systematic effects associated to specific cameras may be related to PSF asymmetries that affect most part of the trajectory.

The observed velocity (Fig. 4c) allowed us to derive an entering speed of 12.2 ± 0.2 km s^{-1} at 76 km of altitude. This speed started to decrease only in the denser layers of the atmosphere below 30 km, just after the brightenings, where it lowered to 10 km s^{-1}. At the end of the luminous path, 21.5 km above the ground, the meteoroid slowed down to 4.0 ± 0.2 km s^{-1}. The estimated value of 76 km for

Downloaded from https://academic.oup.com/mnras/article/501/1/1215/5998250 by Biblioteca Scienze Tecnologiche user on 21 March 2022

the beginning height of the observed trajectory is in close agreement with experimental and simulated data presented in Vida, Brown & Campbell-Brown (2018) for fireballs of asteroidal origin with a low entry speed ($<13\,\mathrm{km\,s^{-1}}$), as seen by low sensitivity all-sky systems. They also found that low velocity meteors decelerate significantly prior to detection of the visible meteor trail. This is the case also for the Cavezzo bolide, for which we estimate a difference between v_∞ and the entry speed of $0.6 \pm 0.3\,\mathrm{km\,s^{-1}}$.

The absolute magnitude light curve is shown in Fig. 4e. In the first 2 s, the brightness grew rapidly, reaching a plateau of about $M = -7.5$ between $t = 2.0$ and 4.7 s, followed by a sudden fading in the last second. Two rapid flares are visible at 3.95 and 4.15 s with absolute magnitudes close to −9.5 and −8.5, respectively, related to the already mentioned fragmentation. The corresponding altitudes are about 32.6 and 30.7 km, respectively, when the meteoroid was still moving at a speed of about $10.1\,\mathrm{km\,s^{-1}}$. Meteoroid fragmentation models usually assume that the fragmentation process starts when the aerodynamic pressure is equal to the mechanical strength S. According to the meteoroid height h and speed V in the main explosion (Foschini 1999), we can estimate a strength of about

$$S = \frac{\gamma - 1}{\gamma} \rho_{sl} V^2 e^{-h/H} \simeq 0.88\ \mathrm{MPa}\,, \quad (1)$$

where $\gamma \sim 1.7$ is the ratio of specific heats, $H \simeq 8\,\mathrm{km}$ is the atmospheric scale height, and $\rho_{\mathrm{sl}} \simeq 1.22\,\mathrm{kg\,m^{-3}}$ is the atmospheric density at sea level. This value is close to the maximum aerodynamic pressure that is attained at a height of about 28.2 km (see Fig. 4d). Since Cavezzo is a stony meteorite, a strength of about 10 MPa could be expected, that is, about one order of magnitude greater. However, it is common to observe fragmentations at aerodynamic pressure well below 1 MPa and even down to few tens of kPa (for example, see Popova et al. 2011; Devillepoix et al. 2019). This evidence suggests a particular weakness of the meteoroid which may be caused, for instance, by fractures already present when it was entering the atmosphere or by porosity of the material.

We estimated the density of the F2 sample by an accurate and precise 3D scanning of the outer surface. Given the measured density of $3.322\,\mathrm{g\,cm^{-3}}$ and by assuming a spherical shape for the entering meteoroid, the computed value for the mass-section ratio D derived by the dynamical model provides, in a purely ablative regime, an estimate of the mass and size before and after the luminous atmospheric transit. The meteoroid pre-atmospheric mass can be estimated to be $3.5 \pm 0.8\,\mathrm{kg}$ ($D = 280 \pm 20\,\mathrm{kg\,m^{-2}}$) with a diameter of $0.13 \pm 0.01\,\mathrm{m}$, while the final mass is $1.5 \pm 0.4\,\mathrm{kg}$ ($D = 210 \pm 20\,\mathrm{kg\,m^{-2}}$). Since there is evidence of possible fragmentation only at a height of about 30 km, we consider our estimation of the initial mass as reliable. On the contrary, the value of the final mass is questionable. Apart from this, the relatively low ablated mass ratio of about 57 per cent could be attributable also to the very low pre-atmospheric speed of $12.8 \pm 0.2\,\mathrm{km\,s^{-1}}$ and to the steep inclination of the trajectory. Compared to the values given in Table 1, the pre-atmospheric mass for the Cavezzo meteorite is the lowest ever reported between 'pedigree' meteorites. From the pre-atmospheric mass and velocity estimates, the impact energy results to be 0.07 ± 0.02 T TNT, which is also the lowest among values given in Table 1.

3.3 Atmospheric data

The knowledge of the atmospheric conditions plays a key role in the computation of the dark flight and strewn-field of meteorite fragments that could be possibly found on the ground. In particular, the wind direction and intensity are the major drivers for the loss of accuracy of these predictions. This effect is even more important in our case, given the small residual mass after ablation and the even smaller expected mass and size of the fragments (order of 100 g/1 cm). For these reasons, we specifically computed the atmospheric state for the Cavezzo area at the time of fall.

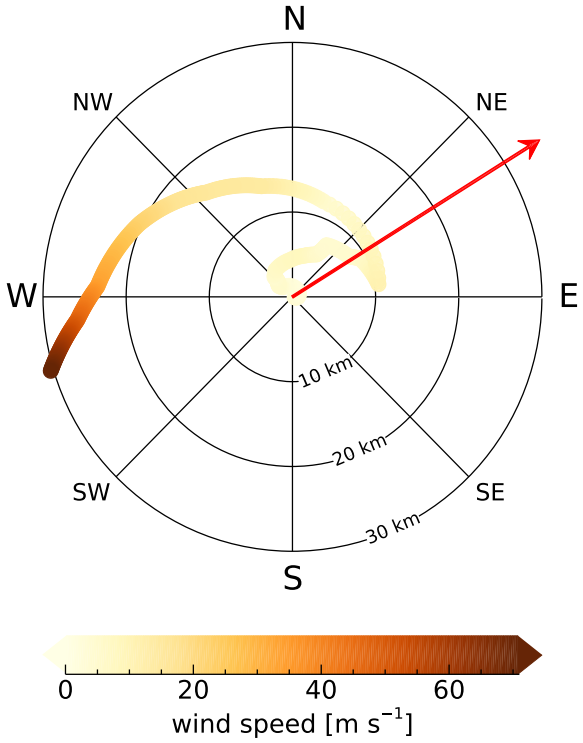


Figure 5. Wind vertical profile at 18 UTC in the Cavezzo area used for the strewn-field computation. The red arrow shows the fireball motion direction on the ground.

Meteorological data came from IOIS (Integrated Observations Ingesting System) elaborated and used at Meteo Expert, a private organization providing meteorological services where weather models are internally developed and applied. All available data, coming from surface, upper air, and remote sensing measurements, are integrated to produce initialization to be perturbed for a limited-area ensemble prediction system. A variational quality control is applied to check data consistency (Steinacker, Mayer & Steiner 2011; Tavolato & Isaksen 2015); the observation is compared with the background and surrounding observations to determine its analysis weight in the system. This procedure is applied to develop perturbed initial data for usual forecast model, that runs at 00, 06, 12, and 18 UTC. However, in our case, as for several other applications including nowcasting, a hourly 3D grid is needed. This grid follows the model's horizontal mesh size at 3.5 km, while in the vertical direction fifty variable-depth levels are used from surface to stratosphere. The scaling of weather parameters at a defined location is made by interpolating values from surrounding grid points, with a correction algorithm which takes into account sub-grid terrain characteristics and local gradients.

3.4 Dark flight and strewn-field

Fig. 5 shows the wind intensity and direction values at 18 UTC in the Cavezzo area as a function of the altitude. The wind was particularly intense at about 22 km, which is the last observed point of the luminous path, reaching a speed of about $28\,\mathrm{m\,s^{-1}}$, and blowing

Downloaded from https://academic.oup.com/mnras/article/501/1/1215/5998250 by Biblioteca Scienze Tecnologiche user on 21 March 2022

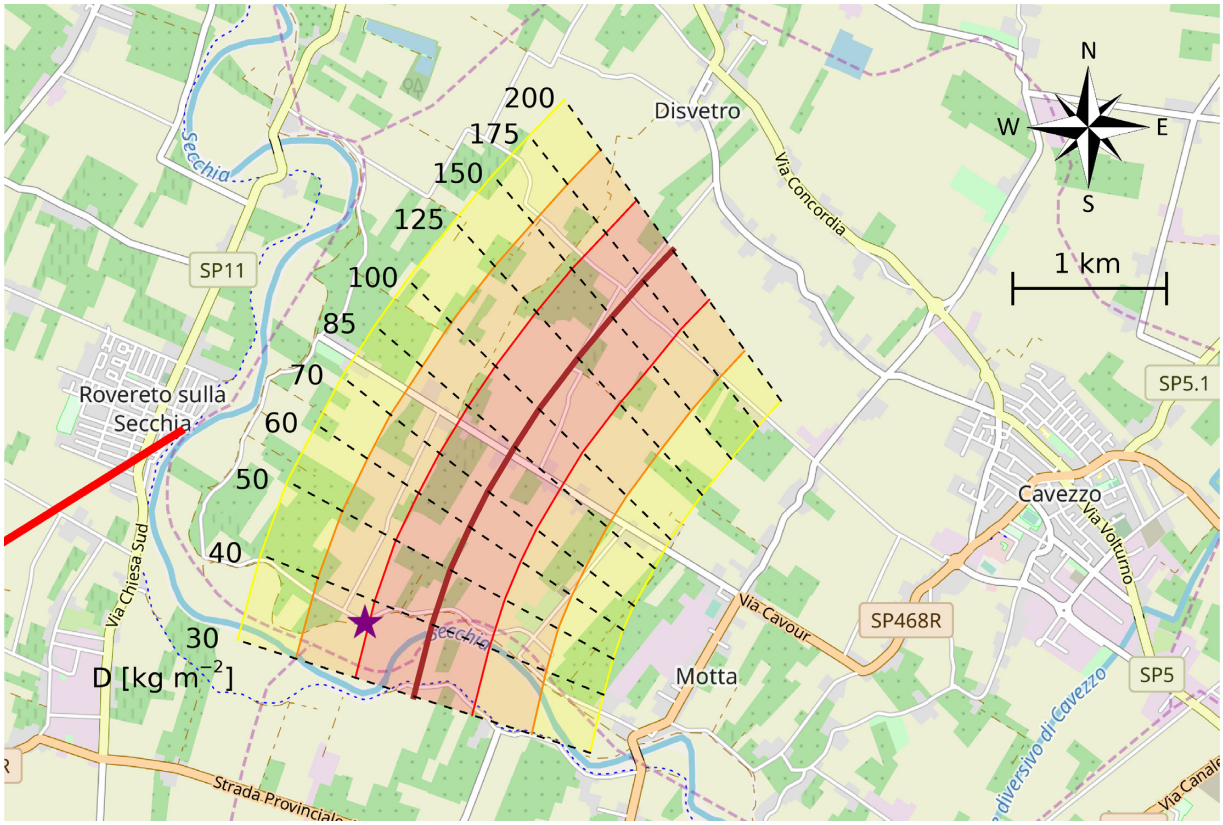


Figure 6. Strewn-field for the Cavezzo meteorite fragments, as a function of different mass-section ratio values (D, dashed black lines) from 30 up to 200 kg m^{-2}. The brown thick line shows the nominal impact point and the shaded areas enclose 1σ (red), 2σ (orange), and 3σ (yellow) uncertainties in the transverse direction. The purple star shows where the two Cavezzo fragments F1 and F2 were recovered, and the thick red line plots the terminal part of the bright flight trajectory, projected on the ground. Background map data copyrighted OpenStreetMap contributors and available from https://www.openstreetmap.org.

at 45° clockwise with respect to the meteoroid motion direction. The wind intensity decreases to reach a speed of about 20 m s^{-1} at 20 km altitude, and is confined below 10 m s^{-1} from 13 km downwards. This led to a significant shift of the strewn-field compared to a situation with zero wind, especially in the transverse direction.

Fig. 6 shows the computed strewn-field for the Cavezzo meteorite, together with the terminal part of the luminous atmospheric trajectory projected on the ground (red line), and the location where the two fragments were recovered (purple star). By assuming that a fragmentation occurred, the impact point computed with a purely ablative model is not representative of the real case. Therefore, we computed the expected impact point for fragments with different mass-section ratios, ranging from $D = 30$ up to 200 kg m^{-2}, which is approximately the final value for the main-mass pure ablation (Section 3.4). The brown thick line shows the most probable impact point as a function of D, while the red/orange/yellow shaded areas represent the 1/2/3σ uncertainty, respectively, in the transverse direction. The 1σ uncertainty in the longitudinal direction can be estimated to be 300 m. Table 4 reports the impact parameters for the sampled D values. The lateral displacement (X) can be as high as 2.3 km for smaller fragments. The expected impact velocity ranges from 28 to 71 m s^{-1}. The position of the recovered fragments lies at the very border of the 1σ transverse interval, in a region where recovered fragments are expected to have mass-section ratio values between 30 and 50 kg m^{-2}. The D values for the two fragments can be estimated to be 30–70 kg m^{-2} for F1 and 35–85 kg m^{-2} for F2, considering that we ignore the orientations of the meteorites during the fall. Therefore, the mass-section ratio for both F1 and F2 is compatible with the predicted values of the dark-flight model. However, since the meteorite very likely fragmented on the ground due to the impact, the D value of the original body remains unknown.

4 A POSSIBLE PROGENITOR OF THE CAVEZZO METEORITE

Using the value of 12.8 ± 0.2 km s^{-1} for the pre-atmospheric velocity, we computed the heliocentric orbit of the meteoroid prior to the impact. The true geocentric speed results to be 5.8 ± 0.5 km s^{-1}. The orbital elements are reported in Table 5. The apparent radiant ($\alpha_a = 6.^\circ5 \pm 0.^\circ2$, $\delta_a = 30.^\circ6 \pm 0.^\circ2$) is located in the Andromeda constellation, while the true radiant ($\alpha_t = 358.^\circ4 \pm 0.^\circ3$, $\delta_t = 24.^\circ4 \pm 0.^\circ3$) is in Pegasus. The computed heliocentric orbit, shown as the red ellipse (nominal value) and shaded area (1σ uncertainty) in Fig. 7, has moderate eccentricity and low inclination on the Ecliptic, with a Tisserand invariant with respect to Jupiter equal to 4.1 ± 0.2, thus, indicating that the progenitor meteoroid was of asteroidal origin.

To find possible progenitor(s) of the Cavezzo meteorite, we followed the procedure described in Carbognani et al. (2020), using the orbital similarity criterion D_N introduced by Valsecchi, Jopek & Froeschle (1999); the NEODyS data base[10] (Chesley & Milani 1999) conveniently lists the secular quantities used in D_N for all Near-Earth

[10]NEODyS-2 data base – https://newton.spacedys.com/~neodys2/propneo/encounter.cond

Downloaded from https://academic.oup.com/mnras/article/501/1/1215/5998250 by Biblioteca Scienze Tecnologiche user on 21 March 2022

Table 4. Data regarding the nominal impact points with different D final values. From top to bottom: final mass-section value, latitude and longitude of the impact point, shift parallel (L) and orthogonal (X) to motion direction of the bright flight and on-ground impact velocity.

	Quantity										
Final D (kg m^2)	30	40	50	60	70	85	100	125	150	175	200
Lat. N impact point (°)	44.8245	44.8287	44.8318	44.8343	44.8364	44.8390	44.8412	44.8441	44.8466	44.8486	44.8504
Long. E impact point (°)	10.9759	10.9773	10.9789	10.9804	10.9819	10.9841	10.9862	10.9893	10.9921	10.9947	10.9971
L (km, ± 0.3)	0.4	0.7	1.0	1.2	1.5	1.8	2.0	2.4	2.7	3.0	3.3
X (km, ± 0.4)	2.3	1.9	1.7	1.5	1.4	1.2	1.1	1.0	0.8	0.8	0.7
$v_{\rm impact}$ (m s^{-1})	28	32	36	39	42	47	51	56	62	66	71

Table 5. Orbital elements (top) and proper elements (bottom) of the Cavezzo meteoroid (left) and of 2013 VC$_{10}$ from NEODyS (right).

Quantity	Cavezzo	2013 VC$_{10}$
Epoch	J2000	MJD59000
Semimajor axis (AU)	1.82 ± 0.22	1.56622
Eccentricity	0.460 ± 0.063	0.365295
Inclination (°)	4.0 ± 1.6	2.044
Long. of ascending node (°)	280.52311 ± 0.00001	224.068
Argument of Perihelion (°)	179.2 ± 4.8	240.264
Longitude of Perihelion (°)	99.7 ± 4.8	104.332
Perihelion passage (JD)	2458849.6 ± 0.5	2458808.1
Perihelion distance (AU)	0.983 ± 0.001	0.9941
Aphelion distance (AU)	2.66 ± 0.41	2.1383
U	0.216 ± 0.001	0.1818
θ (°)	22.96 ± 0.30	24.8358
ϕ (°)	175.90 ± 0.69	171.49
$\lambda_\oplus$ (°)	100.52311 ± 0.00001	104.986

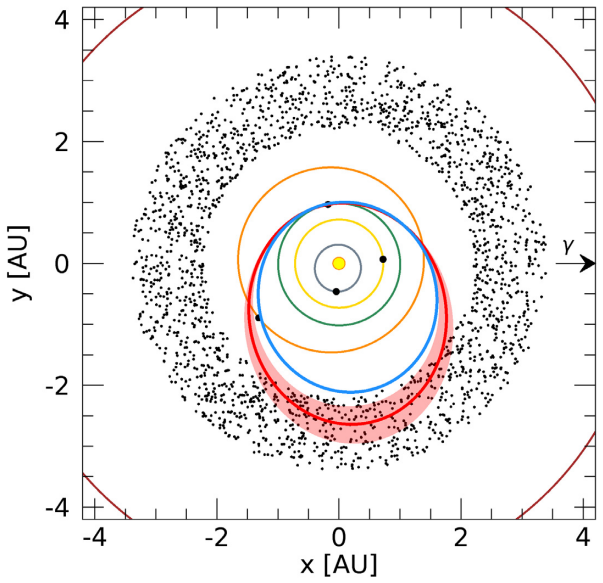


Figure 7. The reconstructed heliocentric orbit for the progenitor meteoroid of the Cavezzo meteorite (red ellipse) as seen from the ecliptic north pole and projected on to the ecliptic plane, together with the 1σ uncertainty band (shaded red area). The blue ellipse plots the 2013 VC$_{10}$ orbit (for which orbital elements are provided by the NEODyS data base). Remaining ellipses plot Solar system planets' orbits up to Jupiter, and the black dots indicate their position along the orbit at the time of the IT20200101 fireball. The black small dots symbolically represent the asteroid Main Belt.

Asteroids (NEAs) for which they are defined (Gronchi & Milani 2001). We use D_N in the form

$$D_N = \sqrt{(U-U_c)^2 + (\cos\theta - \cos\theta_c)^2 + \Delta\xi^2}\,, \qquad (2)$$

with:

$$\Delta\xi^2 = \min\left[\Delta\phi_I^2 + \Delta\lambda_I^2,\, \Delta\phi_{II}^2 + \Delta\lambda_{II}^2\right]$$

$$\begin{cases} \Delta\phi_I = 2\sin\frac{\phi-\phi_c}{2} \\ \Delta\phi_{II} = 2\sin\frac{180^\circ+\phi-\phi_c}{2} \\ \Delta\lambda_I = 2\sin\frac{\lambda_\oplus-\lambda_{\oplus,c}}{2} \\ \Delta\lambda_{II} = 2\sin\frac{180^\circ+\lambda_\oplus-\lambda_{\oplus,c}}{2}\,. \end{cases}$$

In the above expressions, U, θ, ϕ, $\lambda_\oplus$ refer to the NEA, and are taken from NEODyS, while $U_c, \theta_c, \phi_c, \lambda_{\oplus,c}$ are those of the Cavezzo meteorite (Table 5). Details on the definition of the variables and on D_N are given in Valsecchi et al. (1999). We looked for NEAs for which $D_N \leq 0.15$. The search resulted in only one candidate, 2013 VC$_{10}$, for which proper elements are given in the last column of Table 5; for the pair Cavezzo-2013 VC$_{10}$, $D_N = 0.115$. The nominal orbit of 2013 VC$_{10}$, projected on to the ecliptic plane, is shown in Fig. 7 (blue ellipse). There is a reasonable similarity between the two orbits, which is more evident if one considers the secular quantities that enter the computation of D_N. On the other hand, the pair Cavezzo-2013 VC$_{10}$ is rather isolated in the 4-dimensional space $U, \theta, \phi, \lambda_\oplus$; this isolation is recognizable even in the 2-dimensional space constituted by the ecliptical radiant coordinates. Fig. 8 shows the radiants of the pair Cavezzo-2013 VC$_{10}$, as well as the radiants of the simulated impactors of Chesley & Spahr (2004), and of the 20 real impactors listed in Granvik & Brown (2018). As discussed in the Appendix of Farnocchia, Bernardi & Valsecchi (2012), the radiant distribution simply reflects the values of the semimajor axis, eccentricity, and inclination of those NEAs whose orbits actually can cross that of the Earth. As a result, NEA impactor radiants are not uniformly distributed in a plot like Fig. 8a, but present concentrations and regions of low density that are even more evident in Fig. 8b. It is in one of the low-density regions that the pair Cavezzo-2013 VC$_{10}$ is located, lending some additional credibility to the possible association.

5 CONCLUSIONS

After less than three years of operations, the PRISMA network, partner of FRIPON, has achieved one of its major objectives, i.e. the recovery of the first Italian meteorite by computation of a precise strewn-field through the analysis of its observational data. Two meteorite fragments, fallen near Cavezzo (Modena) on New Year's Day 2020, weighing 3.1 and 52.2 g, were recovered three days after the fall as a result of a dedicated field search and thanks to the involvement of local people. They were found at a distance

Downloaded from https://academic.oup.com/mnras/article/501/1/1215/5998250 by Biblioteca Scienze Tecnologiche user on 21 March 2022

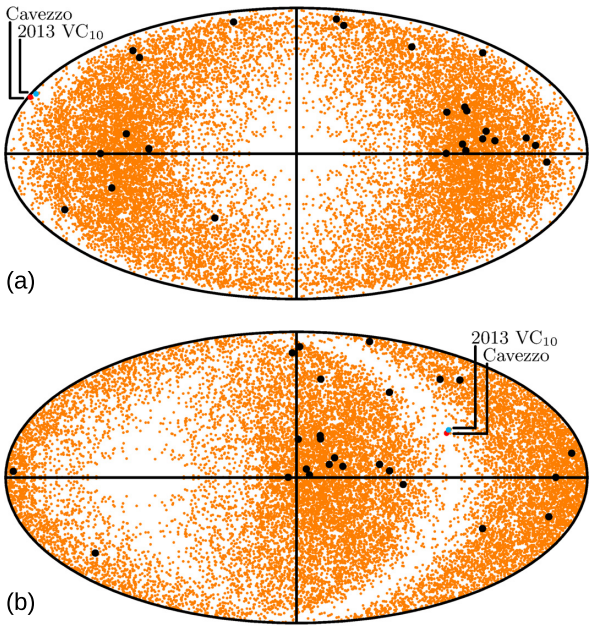


Figure 8. The radiants of the Cavezzo meteoroid (red dot) and of 2013 VC_{10} (cyan dot) in an equal area projection of the sky centred on the apex of the Earth motion (a) and on the opposition (b); the angular coordinates are ecliptic longitude minus the longitude of the Sun, and ecliptic latitude. The orange dots are the radiants of the simulated impactors of Chesley & Spahr (2004), while the black dots are the radiants of the 20 meteorites listed in Granvik & Brown (2018).

of 400 m from the nominal computed position, very close to the 1σ uncertainty value. These fragments were immediately recognized as freshly fallen meteorites, a fact that has been confirmed by the unquestionable presence of short-lived cosmogenic radioisotopes (such as ^{48}V, half-life of 15.97 d) measured with a very sensitive γ-ray detector at the INAF Monte dei Cappuccini Laboratory in Torino. The analyses carried out at the Department of Earth Sciences of the Firenze University highlighted strong differences between the two specimens and led the Nomenclature Committee of the Meteoritical Society to approve the classification proposal of anomalous L5 chondrite.

The computed orbital parameters and the value of the Tisserand invariant ($T_J = 4.1 \pm 0.2$) are typical of a NEA with an aphelion located in the inner part of the main belt. The orbital elements, compared with the ones of known NEAs from the NEODyS data base, show that only one object among those, namely 2013 VC_{10}, is compatible with the Cavezzo meteoroid. Moreover, the radiants of both objects are located in a low-density region of NEA impactors, thus, lending additional credibility to the association.

The associated fireball trajectory, observed by many eyewitnesses, was characterized by an entry velocity of 12.2 ± 0.2 km s^{-1} and by a high-inclination angle of $68\overset{\circ}{.}4 \pm 0\overset{\circ}{.}3$. The luminous path started at a height of 75.9 ± 0.2 km and reached 21.5 ± 0.1 km, after travelling approximately 59 km in 5.6 s. The absolute magnitude reached a minimum of -9.5 at 32.6 km of altitude, where a bright flash was seen, very likely indicating a fragmentation and followed by a second flash reaching -8.5. In the brightest part of the trajectory, the mean absolute magnitude was around -7.5. By assuming a purely ablative regime, a spherical form of the meteoroid, and given the measured meteorite bulk density of 3.322 g cm^{-3}, the estimated residual mass is 1.5 ± 0.4 kg.

The pre-atmospheric mass and velocity of 3.5 ± 0.8 kg and 12.8 ± 0.2 km s^{-1}, respectively, leading to a total impact energy of less than 0.07 T TNT, together with the brightest absolute magnitude reached, are the lowest among those estimated for the 35 meteorites with 'pedigree' recovered so far, as listed in Table 1. Currently, this recovery can be considered to date the most challenging in terms of size and magnitude of the associated event, proving the efficiency of the network and of our reduction pipeline even in such demanding conditions.

ACKNOWLEDGEMENTS

PRISMA is the Italian network for systematic surveillance of meteors and atmosphere. It is a collaboration initiated and coordinated by the Italian National Institute for Astrophysics (INAF) that counts members among research institutes, universities, associations, and schools. The complete list of PRISMA members is available here: http://www.prisma.inaf.it. PRISMA was funded by 2016/0476 and 2019/0672 *Research and Education* grants from Fondazione Cassa di Risparmio di Torino and by a 2016 grant from Fondazione Agostino De Mari (Savona). PRISMA data are hosted by the INAF research e-infrastructure project IA2 (Italian Center for Astronomical Archives).

FRIPON was funded by the ANR grant no.13-BS05-0009-03, carried by the Paris Observatory, Muséum National d'Histoire Naturelle, Paris-Saclay University, and Institut Pythéas (LAM-CEREGE). FRIPON data are hosted and processed at Institut Pythéas SIP (Service Informatique Pythéas), and a mirror is hosted at IMCCE (Institut de Mécanique Céleste et de Calcul des Éphémérides / Paris Observatory) with the help of IDOC (Integrated Data and Operation Center), supported by CNRS and CNES.

The PRISMA collaboration is grateful to Mr. Davide Gaddi, who recovered the meteorite fragments, allowed for the analysis of the samples, and eventually decided to donate them to INAF.

The authors are very grateful to Leonard Kornoš for the useful comments that greatly improved the manuscript and to Rebecca O'Brien for the precious work of language revision.

Background map data for Fig. 6 copyrighted OpenStreetMap contributors and available from https://www.openstreetmap.org, distributed under the Open Data Commons Open Database License (https://opendatacommons.org/licenses/odbl/).

DATA AVAILABILITY

PRISMA data underlying this article will be shared on reasonable request to the corresponding author.

REFERENCES

Audureau Y. et al., 2014, in Rault J.-L., Roggemans P., eds, Proc. 33th International Meteor Conference. International Meteor Organization, Hove, Belgium, p. 39

Barghini D., Gardiol D., Carbognani A., 2019a, in Proc. 37th International Meteor Conference Pezinok-Modra. International Meteor Organization, Hove, Belgium, p. 41

Barghini D., Gardiol D., Carbognani A., Mancuso S., 2019b, A&A, 626, A105

Bischoff A. et al., 2011, Meteorit. Planet. Sci., 46, 793

Bischoff A., Dyl K. A., Horstmann M., Ziegler K., Wimmer K., Young E. D., 2013, Meteorit. Planet. Sci., 48, 628

Bischoff A. et al., 2017, Meteorit. Planet. Sci., 52, 1683

Bischoff A. et al., 2019, Geochemistry/Chem. Erde, 79, 125525

Bland P. A. et al., 2009, Science, 325, 1525

Downloaded from https://academic.oup.com/mnras/article/501/1/1215/5998250 by Biblioteca Scienze Tecnologiche user on 21 March 2022

Bland P. A. et al., 2016, in 79th Annual Meeting of the Meteoritical Society. Lunar and Planetary Institute, Houston, Texas, USA, p. 6265
Borovička J., 1990, Bull. Astron. Inst. Czechoslov., 41, 391
Borovička J., Charvát Z., 2009, A&A, 507, 1015
Borovička J., Kalenda P., 2003, Meteorit. Planet. Sci., 38, 1023
Borovička J., Spurný P., Keclikova J., 1995, A&AS, 112, 173
Borovička J., Popova O. P., Nemtchinov I. V., Spurný P., Ceplecha Z., 1998, A&A, 334, 713
Borovička J., Spurný P., Kalenda P., Tagliaferri E., 2003a, Meteorit. Planet. Sci., 38, 975
Borovička J. et al., 2003b, Meteorit. Planet. Sci., 38, 1005
Borovička J. et al., 2013a, Meteorit. Planet. Sci., 48, 1757
Borovička J., Spurný P., Brown P., Wiegert P., Kalenda P., Clark D., Shrbený L., 2013b, Nature, 503, 235
Borovička J. et al., 2015, Meteorit. Planet. Sci., 50, 1244
Borovička J., Popova O., Spurný P., 2019, Meteorit. Planet. Sci., 54, 1024
Bouvier A., Gattacceca J., Agee C., Grossman J., Metzler K., 2017, Meteorit. Planet. Sci., 52, 2284
Brown P., Ceplecha Z., Hawkes R. L., Wetherill G., Beech M., Mossman K., 1994, Nature, 367, 624
Brown P., Pack D., Edwards W. N., Revelle D. O., Yoo B. B., Spalding R. E., Tagliaferri E., 2004, Meteorit. Planet. Sci., 39, 1781
Brown P. et al., 2011, Meteorit. Planet. Sci., 46, 339
Brown P. G. et al., 2000, Science, 290, 320
Brown P. G., Revelle D. O., Tagliaferri E., Hildebrand A. R., 2002, Meteorit. Planet. Sci., 37, 661
Brown P. G. et al., 2013, Nature, 503, 238
Brown P. G. et al., 2019, Meteorit. Planet. Sci., 54, 2027
Carbognani A. et al., 2020, Eur. Phys. J. Plus, 135, 255
Ceplecha Z., 1961, Bull. Astron. Inst. Czechoslov., 12, 21
Ceplecha Z., 1987, Bull. Astron. Inst. Czechoslov., 38, 222
Ceplecha Z., 1996, A&A, 311, 329
Ceplecha Z., Revelle D. O., 2005, Meteorit. Planet. Sci., 40, 35
Chesley S. R. , Milani A., 1999, BAAS, 31, 1117
Chesley S. R., Spahr T. B., 2004, in Belton M., Morgan T. H., Samarasinha N., Yeomans D. K., eds, Mitigation of Hazardous Comets and Asteroids. Cambridge Univ. Press, Cambridge, UK, p. 22
Clark D. L., Wiegert P. A., 2011, Meteorit. Planet. Sci., 46, 1217
Colas F. et al., 2014, in Proc. 33th International Meteor Conference. International Meteor Organization, Hove, Belgium, p. 18
Colas F. et al., 2020, A&A, 644, A53
Colombetti P., Taricco C., Bhandari N., Sinha N., Di Martino M., Cora A., Vivaldo G., 2013, Nucl. Instrum. Methods Phys. Res. A, 718, 140
Devillepoix H. A. R. et al., 2018, Meteorit. Planet. Sci., 53, 2212
Devillepoix H. A. R. et al., 2019, MNRAS, 483, 5166
Dyl K. A. et al., 2016, Meteorit. Planet. Sci., 51, 596
Farnocchia D., Bernardi F., Valsecchi G. B., 2012, Icarus, 219, 41
Ferus M. et al., 2020, Icarus, 341, 113670
Foschini L., 1999, A&A, 342, L1
Gardiol D., Cellino A., Di Martino M., 2016, in Proc. 35th International Meteor Conference Egmond. International Meteor Organization, Hove, Belgium, p. 76
Gardiol D. et al., 2019, in Proc. 37th International Meteor Conference Pezinok-Modra. International Meteor Organization, Hove, Belgium, p. 81
Gattacceca J., Bouvier A., Grossman J., Metzler K., Uehara M., 2019, Meteorit. Planet. Sci., 54, 469
Gattacceca J., MCcubbin F. M., Bouvier A., Grossman J., 2020, Meteorit. Planet. Sci., 55, 460
Gounelle M., Spurný P., Bland P. A., 2006, Meteorit. Planet. Sci., 41, 135
Granvik M., Brown P., 2018, Icarus, 311, 271
Gronchi G. F., Milani A., 2001, Icarus, 152, 58
Haack H. et al., 2012, Meteorit. Planet. Sci., 47, 30
Haack H. et al., 2019, Meteorit. Planet. Sci., 54, 1853
Halliday I., Griffin A. A., Blackwell A. T., 1981, Meteoritics, 16, 153
Hildebrand A. R., McCausland P. J. A., Brown P. G., Longstaffe F. J., Russell S. D. J., Tagliaferri E., Wacker J. F., Mazur M. J., 2006, Meteorit. Planet. Sci., 41, 407
Hildebrand A. R. et al., 2009, in Lunar and Planetary Science Conference. Lunar and Planetary Institute, Houston, Texas, USA, p. 2505
Hunter J. D., 2007, Comput. Sci. Eng., 9, 90
Jeanne S. et al., 2019, A&A, 627, A78
Jenniskens P. et al., 2009, Nature, 458, 485
Jenniskens P. et al., 2012, Science, 338, 1583
Jenniskens P. et al., 2014, Meteorit. Planet. Sci., 49, 1388
Jenniskens P. et al., 2019, Meteorit. Planet. Sci., 54, 699
Jenniskens P. et al., 2020, Meteorit. Planet. Sci., 55, 535
Kalenichenko V. V., 2006, A&A, 448, 1185
Knapic C., De Marco M., Smareglia R., Molinaro M., 2014, Astronomical Data Analysis Software and Systems XXIII. Astron. Soc. Pac., Orem, Utah, USA, p. 131
Kohout T. ¡. et al., 2017, Meteorit. Planet. Sci., 52, 1525
Kruijer T. S., Kleine T., Borg L. E., 2020, Nat. Astron., 4, 32
Llorca J. et al., 2005, Meteorit. Planet. Sci., 40, 795
McCrosky R. E., Posen A., Schwartz G., Shao C. Y., 1971, J. Geophys. Res., 76, 4090
Milley E. P., Hildebrand A. R., Brown P. G., Noble M., Sarty G., Ling A., Maillet L. A., 2010, in GeoCanada 2010, GeoConvention, Calgary, Alberta, Canada
Palotai C., Sankar R., Free D. L., Howell J. A., Botella E., Batcheldor D., 2019, MNRAS, 487, 2307
Popova O., Borovička J., Hartmann W. K., Spurný P., Gnos E., Nemtchinov I., Trigo-Rodríguez J. M., 2011, Meteorit. Planet. Sci., 46, 1525
Popova O. P. et al., 2013, Science, 342, 1069
Revelle D. O., Brown P. G., Spurný P., 2004, Meteorit. and Planet. Sci., 39, 1605
Sansom E. K. et al., 2020, Meteorit. and Planet. Sci., 55, 2157
Shaddad M. H. et al., 2010, Meteorit. Planet. Sci., 45, 1557
Simon S. B., Grossman L., Clayton R. N., Mayeda T. K., Schwade J. R., Sipiera P. P., Wacker J. F., Wadhwa M., 2004, Meteorit. Planet. Sci., 39, 625
Spurný P., 1994, Planet. Space Sci., 42, 157
Spurný P., Heinlein D., Oberst J., 2002, in Warmbein B., ed., ESA Special Publication Vol. 500, Asteroids, Comets, and Meteors: ACM 2002. European Space Agency, Paris, France, p. 137
Spurný P., Oberst J., Heinlein D., 2003, Nature, 423, 151
Spurný P., Borovička J., Kac J., Kalenda P., Atanackov J., Kladnik G., Heinlein D., Grau T., 2010, Meteorit. Planet. Sci., 45, 1392
Spurný P., Bland P. A., Shrbený L., Towner M. C., Borovička J., Bevan A. W. R., Vaughan D., 2011, Meteorit. Planet. Sci. Suppl., 74, 5101
Spurný P. et al., 2012, Meteorit. Planet. Sci., 47, 163
Spurný P., Haloda J., Borovička J., Shrbený L., Halodová P., 2014, A&A, 570, A39
Spurný P., Borovička J., Haloda J., Shrbeny L., Heinlein D., 2016, in 79th Annual Meeting of the Meteoritical Society. Lunar and Planetary Institute, Houston, Texas, USA, p. 6221
Spurný P., Borovička J., Baumgarten G., Haack H., Heinlein D., Sørensen A. N., 2017a, Planet. Space Sci., 143, 192
Spurný P., Borovička J., Mucke H., Svoreň J., 2017b, A&A, 605, A68
Spurný P., Bland P. A., Borovička J., Towner M. C., Shrbeny L., Bevan A. W. R., Vaughan D., 2019, in Meteoroids 2019. Comenius University, Bratislava, Slovakia, p. 6369
Spurný P., Borovička J., Shrbený L. ¡., 2020, Meteorit. Planet. Sci., 55, 376
Steinacker R., Mayer D., Steiner A., 2011, Mon. Weather Rev., 139, 3974
Tavolato C., Isaksen L., 2015, Q. J. R. Meteorol. Soc., 141, 1514
Taricco C., Bhandari N., Cane D., Colombetti P., Verma N., 2006, J. Geophys. Res., 111, A08102
Trigo-Rodríguez J. M., Borovička J., Spurný P., Ortiz J. L., Docobo J. A., Castro-Tirado A. J., Llorca J., 2006, Meteorit. Planet. Sci., 41, 505
Trigo-Rodríguez J. M. et al., 2015, MNRAS, 449, 2119
Tóth J. et al., 2015, Meteorit. Planet. Sci., 50, 853
Unsalan O. et al., 2019, Meteorit. Planet. Sci., 54, 953
Valsecchi G. B., Jopek T. J., Froeschle C., 1999, MNRAS, 304, 743
Vida D., Brown P. G., Campbell-Brown M., 2018, MNRAS, 479, 4307

Downloaded from https://academic.oup.com/mnras/article/501/1/1215/5998250 by Biblioteca Scienze Tecnologiche user on 21 March 2022

Welten K. C., Meier M. M. M., Caffee M. W., Nishiizumi K., Wieler R., Jenniskens P., Shaddad M. H., 2010, Meteorit. Planet. Sci., 45, 1728
Wilson G., McCausland P., 2012, Can. J. Earth Sci., 50, 4

[1]*INAF – Osservatorio Astrofisico di Torino, Via Osservatorio 20, I-10025 Pino Torinese, TO, Italy*
[2]*Dipartimento di Fisica – Universitá degli Studi di Torino, Via Pietro Giuria 1, I-10125 Torino, TO, Italy*
[3]*INAF – Osservatorio di Astrofisica e Scienza dello Spazio, Via Piero Gobetti 93/3, I-40129 Bologna, BO, Italy*
[4]*INAF – Osservatorio Astronomico d'Abruzzo, Via Mentore Maggini SNC, Localitá Collurania, I-64100 Teramo, TE, Italy*
[5]*INAF – Osservatorio Astronomico di Trieste, Via Giambattista Tiepolo 11, I-10134 Trieste, TS, Italy*
[6]*Dipartimento di Scienze della Terra – Universitá degli Studi di Firenze, Via Giorgio La Pira, 4, I-50121 Firenze, FI, Italy*
[7]*INAF – Istituto di Astrofisica e Planetologia Spaziali, Via del Fosso del Cavaliere 100, I-00133 Roma, RM, Italy*
[8]*Osservatorio Astronomico del Righi, Via Mura delle Chiappe 44R, I-16136 Genova, GE, Italy*
[9]*Meteo Expert, Via Giovanni Frova, 34, I-20092 Cinisello Balsamo, MI, Italy*
[10]*IFAC – CNR, Via Madonna del Piano 10, I-50019 Sesto Fiorentino, FI, Italy*
[11]*IMCCE, Observatoire de Paris, PSL Research University, CNRS UMR 8028, Sorbonne Université, Université de Lille, 77 av. Denfert-Rochereau, F-75014 Paris, France*
[12]*Institut de Minéralogie, Physique des Matériaux et Cosmochimie (IMPMC), Muséum National d'Histoire Naturelle, CNRS UMR 7590, Sorbonne Université, F-75005 Paris, France*
[13]*GEOPS – Géosciences, CNRS, Université Paris-Saclay, F-91405 Orsay, France*
[14]*Service Informatique Pythéas (SIP) CNRS – OSU Institut Pythéas – UMS 3470, F-13009, Marseille, France*
[15]*Aix Marseille Université, CNRS, IRD, Coll France, INRA, CEREGE, F-13007, Marseille, France*
[16]*International Meteor Organization , B-2540 Hove, Belgium*
[17]*Aix Marseille Université, CNRS, CNES, LAM, F-13007, Marseille, France*
[18]*La Torre del Sole, Via Caduti sul Lavoro 2, I-24030 Brembate di Sopra, BG, Italy*
[19]*Associazione Astrofili Bisalta, Via Gino Eula 23, I-12013 Chiusa di Pesio, CN, Italy*
[20]*Associazione Sky Sentinel, Via Giovanni Leone 36, I-81020 San Nicola la Strada, CE, Italy*
[21]*Meteoriti Italia APS, Via Fusina 6, I-32032 Feltre, BL, Italy*
[22]*GAMP – Osservatorio Astronomico Montagna Pistoiese, I-51028 San Marcello Piteglio, PT, Italy*
[23]*Gruppo Astrofili Antares, Via Garibaldi 12, I-48033 Cotignola, RA, Italy*
[24]*INAF – Osservatorio Astronomico di Brera, Via Brera 28, I-20121 Milano, MI, Italy*
[25]*Associazione Astronomica del Rubicone, Via Palmiro Togliatti 5, I-47039 Savignano sul Rubicone, FC, Italy*
[26]*INAF – Osservatorio Astrofisico di Catania, Via Santa Sofia 78, I-95123 Catania, CT, Italy*
[27]*SpaceDyS, Via Mario Giuntini 63, I-56023 Navacchio di Cascina, PI, Italy*
[28]*Osservatorio Polifunzionale del Chianti – Universitá di Firenze, Strada Provinciale Castellina in Chianti, I-50021 Barberino Val D'Elsa, FI, Italy*
[29]*Associazione Astrofili Urania, Localitá Bric del Colletto 1, I-10062 Luserna San Giovanni, TO, Italy*
[30]*INAF – Osservatorio Astronomico di Capodimonte, Salita Moiariello 16, I-80131 Napoli, NA, Italy*
[31]*Associazione Astrofili Tethys – Planetario e Osservatorio Astronomico di Ca' del Monte, Localitá Ca' del Monte, I-27050 Cecima, PV, Italy*
[32]*INFN – Sezione di Torino, Via Pietro Giuria 1, I-10125 Torino, TO, Italy*
[33]*Associazione Culturale Googol, Via Filippo Brunelleschi 21, I-43100 Parma, PR, Italy*
[34]*INAF – Osservatorio Astronomico di Padova, Vicolo dell'Osservatorio 5, I-35122 Padova, PD, Italy*
[35]*Fondazione GAL Hassin – Centro Internazionale per le Scienze Astronomiche, Via della Fontana Mitri, I-90010 Isnello, PA, Italy*
[36]*Planetarium Pythagoras, Via Margherita Hack, I-89125 Reggio Calabria, RC, Italy*
[37]*Dipartimento di Matematica e Fisica – Universitá del Salento, Via Per Arnesano, I-73100 Lecce, LE, Italy*
[38]*Fondazione Museo Civico di Rovereto – Osservatorio Astronomico di Monte Zugna, Localitá Zugna, I-38068 Rovereto, TN, Italy*
[39]*Liceo Statale 'Arturo Issel', Via Fiume 42, I-17024 Finale Ligure, SV, Italy*
[40]*Gruppo Astrofili Monti Lepini – Osservatorio Astronomico e Planetario di Gorga, I-00030 Gorga, RM, Italy*
[41]*Scuola di Scienze e Tecnologie – Universitá di Camerino, sezione Geologia, via Gentile III da Varano, I-62032 Camerino, MC, Italy*
[42]*INAF – Istituto di Radioastronomia, Via Piero Gobetti 101, I-40129 Bologna, BO, Italy*
[43]*Gruppo Astrofili Montelupo Fiorentino, Piazza Vittorio Veneto 10, I-50056 Montelupo Fiorentino, FI, Italy*
[44]*Dipartimento di Fisica e Astronomia – Universitá di Padova, Vicolo dell'Osservatorio 3, I-35122 Padova, PD, Italy*
[45]*Osservatorio Astrofisico R.P. Feynman, I-73034 Gagliano del Capo, LE, Italy*
[46]*Osservatorio Astronomico Sirio, Piazzale Anelli, I-70013 Castellana Grotte, BA, Italy*
[47]*Osservatorio Astronomico di Sormano, Localitá Colma di, I-22030 Sormano, CO, Italy*
[48]*INAF – Osservatorio Astrofisico di Arcetri, Largo Enrico Fermi 5, I-50125 Firenze, FI, Italy*
[49]*Associazione Astrofili di Piombino – Osservatorio Astronomico di Punta Falcone, Punta Falcone, I-57025 Piombino, LI, Italy*
[50]*Museo di Storia Naturale – Universitá degli Studi di Firenze, Sistema Museale di Ateneo, Via Giorgio La Pira, 4, I-50121 Firenze, FI, Italy*
[51]*INAF – Osservatorio Astronomico di Cagliari, Via della Scienza 5, I-09047 Cuccuru Angius, Selargius, CA, Italy*
[52]*CIRA – Centro Italiano Ricerche Aerospaziali, Via Maiorise SNC, I-81043 Capua, CE, Italy*
[53]*Astrobioparco Oasi di Felizzano, Strada Fubine 79, I-15023 Felizzano, AL, Italy*
[54]*Associazione Ravennate Astrofili Rheyta, Viale Santi Baldini 4/a, I-48121, Ravenna, RA, Italy*
[55]*Dipartimento di Fisica e Astronomia – Universitá degli Studi di Firenze, Via Sansone 1, I-50019 Sesto Fiorentino, FI, Italy*
[56]*IIS 'E.Fermi' di Montesarchio, Via Vitulanese, I-82016 Montesarchio, BN, Italy*
[57]*Liceo Scientifico Statale 'G.B. Quadri', Viale Giosué Carducci 17, I-36100 Vicenza, VI, Italy*
[58]*Dipartimento di Ingegneria Civile – Universitá degli Studi di Trento, Ambientale e Meccanica, Via Mesiano 77, I-38123 Trento, TN, Italy*
[59]*Liceo Scientifico A. Pacinotti, Via XV Giugno SNC, I-19123 La Spezia, SP, Italy*
[60]*Dipartimento di Scienze Ambientali, Informatica e Statistica, Universitá Ca'Foscari di Venezia,, Via Torino 155, I-30172 Mestre Venezia, VE, Italy*
[61]*Museo del Cielo e della Terra, Vicolo Baciadonne 1, I-40017 San Giovanni in Persiceto, BO, Italy*
[62]*Associazione Astrofili Paolo Maffei, Strada Cerruti 39, I-06131 San Marco, Perugia, PG, Italy*
[63]*Dipartimento di Scienze e Innovazione Tecnologica – Universitá del Piemonte Orientale, Viale Teresa Michelin 11, I-15121 Alessandria, AL, Italy*
[64]*Osservatorio Astronomico Giuseppe Piazzi, Localitá San Bernardo, I-23026 Ponte in Valtellina, SO, Italy*
[65]*Liceo Scientifico Statale P. Paleocapa, Via Alcide De Gasperi 19, I-45100 Rovigo, RO, Italy*
[66]*Osservatorio Astronomico Bobhouse, Via Giuseppe Tomasi P.pe di Lampedusa 9, I-90147 Palermo, PA, Italy*

This paper has been typeset from a TEX/LATEX file prepared by the author.

Downloaded from https://academic.oup.com/mnras/article/501/1/1215/5998250 by Biblioteca Scienze Tecnologiche user on 21 March 2022